Published in final edited form as:
Cell Host Microbe. 2013 July 17; 14(1): 104–115. doi:10.1016/j.chom.2013.06.005.

A microscale human liver platform that supports the hepatic stages of *Plasmodium falciparum* and *vivax*

Sandra March[1,6], **Shengyong Ng**[2], **Soundarapandian Velmurugan**[3], **Ani Galstian**[1,6], **Jing Shan**[1], **David Logan**[6], **Anne Carpenter**[6], **David Thomas**[6], **B. Kim Lee Sim**[3], **Maria M. Mota**[4], **Stephen L. Hoffman**[3], and **Sangeeta N. Bhatia**[1,5,6,*]

[1]Health Sciences and Technology/Institute for Medical Engineering and Science, Massachusetts Institute of Technology, Cambridge, MA, 02139, United States of America

[2]Department of Biological Engineering, Massachusetts Institute of Technology, Cambridge, MA, 02139, United States of America

[3]Sanaria Inc., Rockville, MD, 20850, United States of America

[4]Unidade de Malária, Instituto de Medicina Molecular, Universidade de Lisboa, 1649-028 Lisboa, Portugal

[5]Howard Hughes Medical Institute, Koch Institute, and Electrical Engineering and Computer Science, Massachusetts Institute of Technology, Cambridge, MA; Department of Medicine, Brigham and Women's Hospital, Boston, MA, 02115, United States of America

[6]Broad Institute, Cambridge, MA, 02142, United States of America

SUMMARY

The *Plasmodium* liver stage is an attractive target for the development of anti-malarial drugs and vaccines, as it provides an opportunity to interrupt the life cycle of the parasite at a critical early stage. However, targeting the liver stage has been difficult. Undoubtedly, a major barrier has been the lack of robust, reliable and reproducible *in vitro* liver stage cultures. Here, we establish the liver stages for both *Plasmodium falciparum* and *Plasmodium vivax* in a microscale human liver platform composed of cryopreserved, micropatterned human primary hepatocytes surrounded by supportive stromal cells. Using this system, we have successfully recapitulated the full liver stage of *P. falciparum* including the release of infected merozoites and infection of overlaid erythrocytes, and also the establishment of small forms in late liver stages of *P. vivax*. Finally, we validate the potential of this platform as a tool for medium-throughput anti-malarial drug screening and vaccine development.

INTRODUCTION

Despite major advances in the prevention and treatment of malaria, this disease continues to be a major global health problem in human populations with ~250 million cases and nearly 1

*Correspondence: sbhatia@mit.edu.

SUPPLEMENTAL DATA
Supplemental data include four figures

million deaths every year (World Health Organization. Global Malaria Programme, 2010). Malaria is transmitted by *Plasmodium* sporozoites after they are injected by an infected mosquito. Uninucleate sporozoites travel to and invade liver hepatocytes, where they mature and multiply to form liver stage schizonts. These schizonts eventually release pathogenic merozoites into the blood, where they invade erythrocytes and lead to the major clinical symptoms, signs, and pathology of the disease. Human malaria is primarily caused by four species of *Plasmodium* parasites. *Plasmodium falciparum* (*P. falciparum*) is the most virulent and causes the vast majority of deaths. *Plasmodium vivax* (*P. vivax*) is less deadly but highly disabling. Notably, some *P. vivax* sporozoites develop into dormant hypnozoites, which remain in the liver and serve as a *P. vivax* reservoir that gives rise to a chronic, relapsing infection and causes significant added clinical and financial burden (Price et al., 2007). Currently, there is a renewed interest and focus on global malaria eradication, and it is now widely recognized that existing tools are insufficient to meet this goal (Alonso, 2011a, 2011b).

In particular, the clinical options that target the liver stages of the parasite life cycle are inadequate. There is only one licensed drug that eliminates hypnozoites only a few drugs that target liver stage parasites, and no licensed malaria vaccines. This problem has been exacerbated by the emergence of drug resistance, and the inability to treat some populations with primaquine, the only currently approved drug with anti-hypnozoite activity (Wells et al., 2010). The *Plasmodium* liver stage is an attractive therapeutic target for the development of both anti-malarial drugs and vaccines, as it provides an opportunity to interrupt the life cycle of the parasite at a critical early stage. Therefore, screening platforms that model the *in vivo Plasmodium* liver stage could be used to advance the pipeline for anti-malarial drug development and also to validate promising liver stage vaccine candidates (Epstein et al., 2011; Plowe et al., 2009).

Studies of rodent *Plasmodium* pathogens (*P. berghei* and *P. yoelii*) have provided important insights, due in part to the capacity to conduct both *in vitro* and *in vivo* assays (Hoffman et al., 1989; Rodrigues et al., 2008; Silvie et al., 2007). Nonetheless, there are essential differences between the rodent and human parasites, such as their antigenic variation and mechanisms of host cell invasion (Carlton et al., 2002; McCutchan et al., 1985). To date, our understanding of the liver stage of human malaria, mainly *P. falciparum* and *P. vivax*, is based in large part on the infection of human hepatoma cell lines (Chattopadhyay et al., 2010; Epstein et al., 2011; Hollingdale et al., 1983; Karnasuta et al., 1995; Sattabongkot et al., 2006). These cell lines, however, display abnormal proliferation, aberrant signaling, dysregulated gene expression, altered host responses to infection, and inadequate CYP450 and drug metabolism activity, and thus do not accurately recapitulate human hepatocyte biology. Furthermore, *in situ* observation of pathogen development in liver cell lines is typically obscured after 6 days in culture, due to the continued proliferation of infected cells (Yokoo et al., 2004). Primary cultured human hepatocytes that exhibit more physiologic human liver functions have been studied previously, albeit less frequently than cell lines, and can support the development of the liver forms of *P. falciparum* and *P. vivax* (Mazier et al., 1985; Mazier et al., 1984; Rodrigues et al., 2008; van Schaijk et al., 2008; Yalaoui et al., 2008). Nonetheless, in the 25 years since these findings were first published, primary hepatocyte systems are rarely employed and difficult to translate to screening platforms due to limited cell availability, and challenges in maintaining their functional phenotype over extended periods of time *in vitro* (Bhatia et al., 1999).

Two recent advances may help overcome the deficiencies of existing *in vitro* liver models. First, several groups have developed methods and novel culture platforms that support the maintenance of primary human hepatocytes (Bhatia et al., 1999; Guguen-Guillouzo and Guillouzo, 2010; LeCluyse et al., 2012). In particular, our group has developed a microliver

platform, which leverages bioengineering techniques to organize primary human hepatocytes amongst supportive stromal cells (Khetani and Bhatia, 2008). Hepatocytes in these micropatterned cocultures (MPCC) exhibit human-specific drug metabolism, retain drug responsiveness and hepatic energy metabolism, secretion of liver-specific proteins, polarize, and do not proliferate. Importantly, the hepatocytes in MPCC maintain a functional phenotype for up to 4-6 weeks, and are compatible with medium-throughput drug screening methods and automated data collection. This platform has been found to be more predictive than existing *in vitro* liver models for generating and identifying human drug metabolites, drug-induced liver toxicity, and supports the persistent replication of hepatitis C virus (Jones et al., 2010; Ploss et al., 2010; Wang et al., 2010). Furthermore, the availability of large cryopreserved lots of human primary hepatocytes means that donor dependent inter-experimental variability can be minimized. Nonetheless, reproducible access to sporozoites is also critical to achieve a practical system. Cryopreservation of large batches of aseptic sporozoites has also now been established for both *P. vivax* (Chattopadhyay et al., 2010) and *P. falciparum* (Epstein et al., 2011) sporozoites.

In this resource report, we demonstrate the feasibility of integrating cryopreserved human hepatocytes in MPCC with cryopreserved *P. falciparum* and *P. vivax* sporozoites to form an *in vitro* platform that supports the liver stages of human malaria infection. This platform offers the potential for automation based on pre-selection of cryopreserved human hepatocyte and sporozoite batches to standardize infection rate, a machine-learning algorithm that enables an automated imaging-based readout of immunofluorescent staining, and generates a positive Z-factor in response to drug exposure. The 96-well, medium-throughput format requires less reagents (drugs, sporozoites) than larger footprint *in vitro* assays or *in vivo* assays such as humanized mice (Vaughan et al., 2012). Collectively, our data document the development and characterization of a highly-reproducible, medium-throughput microscale human liver platform that may aid in the development of safe and efficacious antimalarial drugs and liver-stage vaccines.

RESULTS

Functional characterization of micropatterned cocultures from cryopreserved primary human hepatocytes

In order to establish an MPCC *in vitro* culture of primary human hepatocytes (Figure 1A) suitable for *Plasmodium* infection, we screened cryopreserved hepatocyes from several individual patient donors to identify those that met the following criteria: a) selective adhesion to collagen type I; b) maintenance of a functional hepatocyte phenotype for up to 3 weeks, as assessed by albumin expression, urea production and CYP450 activity; and c) expression of the previously identified *Plasmodium* host entry factor, CD81 (Silvie et al., 2003). We identified eight donor sources of cryopreserved human hepatocytes that were plateable on collagen I and that displayed typical hepatocyte morphology, including the presence of bile canaliculi (Figure S1). Seven of these sample sets demonstrated functional capacity in culture, as quantified by their production of albumin and urea, and also exhibited CYP450 activity for up to 3 weeks (Figure 1B). We next quantified the expression of the host entry factor CD81 on hepatocytes from each of the seven donors at the day of infection. Four of these samples (Donors 2, 3, 7 and 8) expressed high levels of CD81 by immunofluorescence (Figure 1D).

Infection of primary human hepatocyte MPCCs with *P. falciparum*

To test whether primary hepatocytes stabilized by culturing in MPCCs can be infected with *P. falciparum*, we exposed MPCCs to cryopreserved *P. falciparum* sporozoites (NF54) (Figure 2A,B). We confirmed productive infection in all 7 donors by staining for HSP70

expression, however, a wide range of infection rates were observed between lots (Figure 1C, **left panel**). Specifically, at day 3 post-infection, the number of HSP70+, *P. falciparum* infected hepatocytes was much higher in donor 7 and 8 samples relative to the other tested lots. Hepatocytes from donors 7 and 8 were selected for further characterization of the model. We also examined the susceptibility of the same donor samples to productive infection by two different rodent species of *Plasmodium*. As shown in Figure 1C, **middle panel**, donor 7 and 8 also exhibit the highest levels of *P. yoelii* infection. However, this correlation was not observed in *P. berghei* (Figure 1C, **right panel**). Overall, infection with *P. berghei* was higher compared with *P. falciparum* and *P. yoelii*, with donor 1 showing slightly higher infection with *P. berghei* than the other donors. Interestingly, high CD81 expression was necessary but not sufficient to support robust infection by *P. falciparum* (Figure 1C and 1D). We next evaluated three different batches of cryopreserved *P. falciparum* sporozoites. As seen in Figure 1F, this experiment confirmed productive infection using sporozoites from three cryopreserved batches, however, infection efficiencies varied across batches. Based on higher infection levels, sporozoites from batch 2 were selected for further characterization of the model. Importantly, we observed higher infection rates when hepatocytes were cultured in the MPCC format as opposed to standard, unpatterned (randomly distributed) monocultures (Figure 1E, Hep Random). MPCCs remained susceptible to *P. falciparum* infection for many weeks after they were patterned; however, infection rates are optimal at day 2 after patterning (data not shown).

Recapitulation of entire *P. falciparum* liver stage in MPCCs

Having established that *P. falciparum* can infect MPCCs, we next sought to establish whether the entire liver stage could be reproduced *in vitro*. The viability of the cryopreserved *P. falciparum* sporozoites was evaluated by assessing their gliding motility (Figure 2C), and by their capacity to traverse across cells using a cell wounding assay (Mota et al., 2001). On average, the addition of 37,000 motile cryopreserved *P. falciparum* sporozoites to 10,000 patterned hepatocytes resulted in 3% rhodamine+, traversed cells (Figure 2D). To quantify the ability of the *P. falciparum* sporozoites to invade hepatocytes, *P. falciparum*-treated MPCCs were fixed 3 hours post-infection(Renia et al., 1988). On average, 10% of hepatocytes contained intracellular cryopreserved *P. falciparum* sporozoites (Figure 2E). The human hepatocyte infection rate, based on the percentage of cells containing HSP70-expressing parasites at day 3 post-infection was 0.2% (Figure 2J). Notably, at this same time point, fresh sporozoites achieved infection rates that were 7- to 13-fold higher (Figure 5A). Representative images of the HSP70-expressing parasites at day 3 and day 5 are shown in Figures 2F and 2G.

The maturation of parasites derived from cryopreserved *P. falciparum* was assessed using three parameters: a) immunostaining the infected cultures with antibodies against two proteins first expressed during late liver stages, PfEBA-175 (erythrocyte-binding antigen, 175 kDa) and PfMSP-1 (merozoite surface protein 1), which indicate full development of the respective schizonts inside the hepatocytes into merozoites; b) the size of HSP70-expressing schizonts, relative to previous reports of *P. falciparum* schizont size during liver stage development; and c) the progression rate, calculated as the percentage of schizont-bearing cells at day 5 relative to day 3. At day 5 post-infection, cryopreserved sporozoites express both PfEBA-175 and PfMSP-1 (Figure 3C). The parasites we observed were similar in size to what has been reported in other *in vitro* settings (approx.10 to 15μm at day 5) (Mazier et al., 1985; van Schaijk et al., 2008), but smaller than those reported *in vivo* (Shortt et al., 1951; Shortt and Garnham, 1948; Vaughan et al., 2012), (Figure 2L and 3B). Importantly, we demonstrated that the rate at which parasites progressed to the schizont stage between day 3 to day 6 post-infection was higher in infected MPCCs (33%) relative to the commonly-used hepatoma line, HC04 (14%) (Figure 2K).

Finally, to demonstrate that hepatic schizonts derived from cryopreserved *P. falciparum* sporozoites could achieve full maturity and release infective merozoites, red blood cells were added to the hepatocyte cultures at day 6 post-infection. After 10 days, Giemsa staining revealed infection of erythrocytes by *P. falciparum* merozoites (Figure 2H and 2I).

Assessing progression of attenuated *P. falciparum* for vaccine applications

The ability of the MPCCs to recapitulate the entire liver stage of *P. falciparum in vitro* highlights the potential to use this platform to study the biology of *P. falciparum* infected hepatocytes. For example, this capability should enable the assessment of candidate pre-erythrocyte malarial vaccines that are based on live attenuated parasites (Annoura et al., 2012; Epstein et al., 2011; Mueller et al., 2005; van Schaijk et al., 2008).

To illustrate the potential use of MPCCs in vaccine development, we compared the infection capacity of a pre-erythrocytic malaria vaccine candidate comprised of cryopreserved, live-attenuated *P. falciparum* sporozoites to that of cryopreserved non-attenuated (wild-type) *P. falciparum* sporozoites. Entry of the attenuated parasites was evaluated relative to the function of non-attenuated parasites. As seen in Figure 3A, entry by both groups of parasites was similar. Late liver-stage development was evaluated at day 5 post-infection. Immunofluorescence staining with EBA-175 and MSP-1 antibodies detected mature schizonts only in MPCCs infected with the non-attenuated sporozoites, whereas MPCCs infected with the live-attenuated sporozoites were positive only for the early liver-stage antigen, LSA-1 (Figure 3C). As expected, schizonts that were established by the non-attenuated sporozoites were larger than the immature forms established by the attenuated sporozoites, where the hepatic stage development is arrested. Figure 3B shows a scatter plot of the range of EEF sizes generated by each group.

Development of a semi-automated, medium-throughput platform for antimalarial applications

We next explored the utility of the MPCCs as a potential anti-malarial drug screening platform. The hepatocyte serves both as the site of antimalarial drug metabolism (or bioactivation) and the host for the parasite. Thus, phenotypic stability of the hepatocyte phenotype and a full drug metabolism repertoire has the potential to capture a full range of drug responses such as efficacy, drug-drug interaction and toxicity (Ploss et al., 2010). MPCCs were established in a 96 well format, infected with *P. falciparum*, and treated with the canonical malaria drug, primaquine. The impact of the drug was evaluated based on its ability to reduce parasite infection relative to control cultures in a multi-day dose. As seen in Figure 4A and 4B, the IC50 for primaquine was approximately 1μM for *P. falciparum* during 3 days in culture. The IC50 for *P. falciparum* in the MPCC was lower compared to the IC50 obtained using unpatterned, monocultures of the hepatoma cell line, HC04 (Figure 4A and 4B). Primaquine is known to act via bioactivation to active daughter metabolites in the liver (Pybus et al., 2012). Thus, the clearance of the parent compound can be used as a proxy for the level of bioactivation in culture. We monitored depletion of primaquine in MPCCs, patterned monocultures of primary hepatocytes only (Hep MP), and the HC04 cell line over two days by high-performance liquid chromatography and found that MPCCs most efficiently cleared primaquine over this time frame (Figure 4C). In order to correlate these macroscopic differences in depletion of a parent compound with the drug metabolism repertoire of these model systems, we then compared the expression levels of 83 human-specific drug metabolism genes. In general, the bulk of hepatocyte drug metabolism genes were expressed at higher levels in the MPCCs (Figure 4E). Of the three major enzymes involved with primaquine metabolism, 2 of the 3 were expressed at higher levels in MPCC than the other systems. In particular, Monoamine oxidase A (MAO-A) which is thought to account for over 75% of primaquine metabolism, was expressed at 4-fold higher than

hepatoma cell lines, suggesting that the platform may offer a more predictive system with which to assay candidate drug performance, including studies of mechanism of action.

Next, to further adapt the microliver platform for medium-throughput screens, we characterized several critical parameters. As seen in Figures 5A and 5B, we found that day-to-day variability of hepatocyte infection using the same batch of cryopreserved sporozoites could be minimized (CV 10%) when compared to the range of infection rates obtained using 3 independent batches of fresh sporozoites (CV 42%). Next, a positive Z-factor (Z'>0), which indicates confidence in separating two normally distributed populations was obtained when primaquine-treated wells (10 μM) were compared to control cultures (Figure 5C). In addition, the reproducibility of a phenotypic assay was assessed by establishing consistent dose-dependent inhibitory effects of two different drugs at three different concentrations in 2 independent experiments (atovaquone and primaquine) (Figure 5D). Furthermore, the magnitude of the inhibitory impact of primaquine was consistent across two independent human hepatocyte donors (Figure S2). Finally, we established and validated an automated image analysis read-out using this platform, following the infection of MPCCs with two different doses of sporozoites. As shown in Figure 5E and Figure S3, the number of parasites detected by automated image acquisition and analysis closely matches the counts obtained using conventional manual fluorescence microscopy.

Infection of MPCCs with *Plasmodium vivax*

Plasmodium vivax differs from *P. falciparum* in several important ways. A key feature of *P. vivax* that underlies its persistence in the population is that the liver acts as a reservoir for dormant hypnozoites or 'small forms' (Cogswell, 1992; Krotoski et al., 1982). These hypnozoites can reactivate after weeks, months, or even years, depending on the strain of *P. vivax* (Dao et al., 2007; Durante Mangoni et al., 2003; Garnham et al., 1975). However, due to a lack of model systems available to investigate this elusive organism, the biology of the dormant form of *P. vivax* is underexplored.

Based on our ability to establish the liver stage of *P. falciparum* in MPCCs, to maintain the hepatocyte phenotype for 4-6 weeks, and the observation that some strains of *P. vivax* can reactivate over a similar time scale, we next explored the feasibility of establishing the liver stages of *P. vivax* in MPCC over time. As for the *P. falciparum* experiments, the viability of the cryopreserved *P. vivax* sporozoites was evaluated by assessing their gliding motility prior to each experiment (Figure 6A). We explored several strains of *P. vivax* including Chesson, a strain known to efficiently form dormant forms and to reactivate at shorter time scales (Hollingdale et al., 1986; Krotoski et al., 1986). Cultures were infected and then fixed at various time points and stained for CSP. Using immunofluorescence microscopy, we analyzed the size distribution and localization of the *P. vivax* forms over a three week period. We readily observed *P. vivax* liver forms in MPCC, including mature, liver-stage schizonts larger than 20μm found at day 6 post-infection (Figure 6C, 6B and Figure S4A-B). In addition, a population of smaller PvCSP-positive forms (<5μM) was detected within MPCCs at all time points, particularly identifiable at 6 and 21 days post-infection (Figure 6A, 6B and Figure S4A-C). The infection efficiency, based on the percentage of hepatocytes containing large and small PvCSP+ forms at day 6 post-infection was 0.013% and 2%, respectively (Figure S4D). Similar numbers of small forms were observed up to day 21 (data not shown). Importantly, 85% of the small forms observed were intracellular, based on immunostaining performed before and after permeabilization (Figure S4C). In contrast, cultures infected with *P. falciparum* contained very few small forms after 15 days in culture, and those were predominantly extracellular (Figure S4E). These *P. vivax* small forms may represent the dormant hypnozoite stage of the parasite life cycle, which are responsible for clinical relapses in *P. vivax* malaria patients; however, further characterization will be required to substantiate this hypothesis. Both small and large forms were observed when

other strains of fresh and frozen *P. vivax* sporozoites were examined (Figure S4A **and data not shown**). Finally, we demonstrated that the MPCC system can support maturation of hepatic *P. vivax* schizonts, based on the detection of the late stage antigen, PvMSP-1, at day 12 post-infection (Figure S4B).

DISCUSSION

In this report, we describe an *in vitro* cell-based platform that recapitulates the human liver stage of *P. falciparum* and *P. vivax* infection. Although some attempts to infect cryopreserved human primary hepatocytes have been described in the past (Meis et al., 1985; Silvie et al., 2004), this source of hepatocytes has not been routinely adopted by the field, to date. The advantages of screening individual donor-derived cryopreserved hepatocytes is paralleled by the successful production of purified, vialed, cryopreserved sporozoites (Chattopadhyay et al., 2010; Epstein et al., 2011; Hoffman et al., 2010). These cryopreserved resources overcome the donor-to-donor variability seen in primary cultured human hepatocyes, as well as infectivity rate variability introduced by different batches of mosquitoes or sporozoites. In addition, the use of cryopreserved components in this platform allows for a reliable source of reagents for use in longitudinal experiments, including screening and subsequent validation. Furthermore, since patterned hepatocyte culture using the MPCC platform can maintain individual patient samples for between 4 and 6 weeks (Khetani and Bhatia, 2008), long-term monitoring of even blood-stage *Plasmodium* infections, analysis of genetic changes acquired inside Anopheles mosquitoes, safety assessment of attenuated sporozoite vaccine candidates, and *in vitro* characterization studies of *P. vivax* hypnozoites are all feasible. Notably, development of vaccines and drugs against this stage of *P. vivax* has been identified as a critically important goal for research to eradicate malaria (Alonso et al., 2011a; Alonso et al., 2011b). Recent publications have highlighted that existing candidate vaccines continue to underperform in clinical trials, and significant “blood breakthrough” of presumably attenuated parasites formulations has been observed (Annoura et al., 2012).

In our experience with disease modeling of drug-induced liver injury and hepatitis C infection, establishing platforms that better reflect host biology is an important first step to determining where existing model systems were lacking (e.g. P450 activity and interferon signaling, respectively). In this case, we have already observed three advantages over *in vitro* hepatoma cultures: 1) sporozoites appear to progress through the parasite life cycle more efficiently in MPCC relative to infected hepatoma cells, offering the potential to improve studies of drugs and sporozoite attenuation strategies that act in the second half of the liver life cycle; 2) MPCC are able to predict differences in infection rates of sporozoites *in vivo* that result from cryopreservation, likely reflecting the presence of critical host factors that are altered in hepatoma cells (Albuquerque et al., 2009; Epiphanio et al., 2008; Prudencio et al., 2008; Rodrigues et al., 2008; Silvie et al., 2003); and 3) MPCCs fabricated from different human hepatocyte donors enable direct comparison of host factors that impact entry of different sporozoite species and strains (e.g. CD81 in *P. yoeli, P. berghei, P. falciparum*), whereas hepatoma cells are typically limited to one or very few donor genotypes. We demonstrated that maintenance of hepatocyte function and expression of the host entry factor CD81 (Silvie et al., 2003) were necessary but not sufficient to obtain adequate levels of infection by *P. falciparum*. This finding suggests the existence of as-yet uncharacterized molecular differences among donors that determine their permissiveness to *Plasmodium* infection. Furthermore, most antimalarial drug development leads identified in red blood cell-based high throughput screens do not require metabolic activation, thus in such cases, screening via the MPCC format might yield the same or higher/lower IC50 predictions, should the candidate compound be cleared rapidly or bioactivated via metabolic pathways (Gamo et al., 2010; Guiguemde et al., 2010)

The infection rates reported in this study using cryopreserved sporozoites are comparable or higher than the ones previously documented with fresh sporozoites, and they are an additional ~10-fold higher when we used fresh sporozoites (Mazier et al., 1985; Mazier et al., 1984; Sattabongkot et al., 2006; van Schaijk et al., 2008). The infection rates of hepatocytes in MPCC is similar in comparison to the infection rates recently reported in HC04 cells which range from 0.4% to 0.06% (Epstein et al., 2011; Sattabongkot et al., 2006); however, in our system the progression rate from one stage of the life cycle to the other was much higher than in HC04, offering the potential for studying later stages of the liver life cycle more efficiently. Nonetheless, our MPCC infection rates remain low relative to those recorded in *in vivo* settings (Shortt et al., 1951; Shortt and Garnham, 1948). Experiments done in mice with *P. yoelii* (Conteh et al., 2010), and nonhuman primates with *P. knowlesi* (Jiang et al., 2009) have demonstrated that intravenous inoculation of only a few non-cryopreserved sporozoites (10 spz) can lead to a productive malaria infection that results in detectable parasitemia in the blood stage. Varying hypotheses have been put forward to explain the discrepancy between model systems. For example, our *in vitro* systems do not provide the host hepatocytes with potentially necessary, physiologically relevant cellular components, such as Kupffer cells or sinusoidal endothelial cells. Further, the MPCC platform conformational cues may be important for EEF growth (e.g. 2D versus 3D). These hypotheses will be explored further.

In conclusion, the ability to support the liver stages of *P. falciparum and P. vivax* parasites in a medium-throughput format offers promise to improve our fundamental understanding of the liver stages of human malaria as well as accelerate the development of drugs and vaccines to aid eradication.

EXPERIMENTAL PROCEDURES

Micropatterned cocultures

12mm coverslips that were placed into tissue culture polystyrene 24-well plates or glass-bottomed 96-well plates were coated homogenously with rat tail type I collagen (50 μg/ml) and subjected to soft-lithographic techniques (Ploss et al., 2010) to pattern the collagen into micro-domains (islands of 500 μm) that mediate selective hepatocyte adhesion. To create MPCCs, cryopreserved primary human hepatocytes were pelleted by centrifugation at 100× g for 6 min at 4 °C, assessed for viability using Trypan blue exclusion (typically 70–90%), and then seeded on collagen-micropatterned plates. The cells were washed with medium 2–3 h later and replaced with human hepatocyte culture medium. 3T3-J2 murine embryonic fibroblasts were seeded (40,000 cells in each well of 24-well plate and 10,000 cells in each well of 96-well plate) in fibroblast medium 3 days later. Fibroblast medium was replaced with human hepatocyte medium 24 h after fibroblast seeding and subsequently replaced daily (Khetani and Bhatia, 2008).

P. falciparum and *P. vivax* sporozoites

Mosquitoes were fed on Pf- and Pv- infected blood as previously described (Chattopadhyay et al., 2010; Epstein et al., 2011). Briefly, *P. falciparum* and *P. vivax* sporozoites were extracted from infected mosquitoes by dissection of their salivary glands and passing the glands back and forth through a 26K G needle fitted to a 1 mL syringe. Following extraction, sporozoites were purified from mosquito salivary gland material contamination and cryopreserved in liquid nitrogen vapor phase (LNVP) (Epstein et al., 2011; Hoffman et al., 2010). Live-attenuated *P. falciparum* sporozoites were attenuated by exposure of PfSPZ-infected mosquitoes to 150 Gy (Epstein et al., 2011; Hoffman et al., 2010).

Infection of MPCCs with *P. falciparum* and *P. vivax*

Typically, infection of MPCCs is conducted two days after hepatocyte seeding, but can also be initiated after longer culture periods. Cryovials containing *P. falciparum* or *P. vivax* were warmed for 30 sec at 37°C, 200 μl of human hepatocyte medium was added and the cryovials were centrifuged for 2 min at 14000× g. 200 μl of the supernatant was aspirated, and the sporozoite pellet was resuspended and diluted accordingly. Each well was infected with a ratio of 3:1 (infective sporozoites:hepatocytes). After incubation at 37°C and 5% CO_2 for 3h, the wells were washed once and fresh medium was added. Media was replaced daily. Samples were fixed on day 3 and 5 post-infection with *P. falciparum*, and days 3, 6, 12, and 21 post-infection with *P. vivax.*

Cell wounding and membrane repair assay

Sporozoite migration through cells can be quantified by the detection of sporozoite-wounded hepatocytes using a cell-impermeant fluorescent tracer macromolecule as previously described (Mota et al., 2001). Briefly, MPCCs were infected with *P. falciparum* in the presence of 1 mg/ml tetramethylrhodamine dextran lysine fixable, 10,000 Da (Sigma). At 3h post-infection, MPCCs were washed thrice with PBS, fixed with 1% paraformaldehyde at room temperature for 20 min, and mounted on glass slides. Migration of sporozoites through cells is quantified by the number of dextran-positive hepatocytes per island.

Double-staining assay for sporozoite entry

At 3 h post-infection, primary human hepatocytes or MPCCs were fixed and stained using a double-staining protocol as previously described (Renia et al., 1988). Briefly, to label extracellular sporozoites, the samples were first fixed with 4% paraformaldehyde for 10min at room temperature, blocked with 2% BSA in PBS, incubated with a primary mouse anti-PfCSP (Sanaria, 1:100) (Nardin et al., 1982), washed thrice in PBS and incubated with a secondary goat anti-mouse AlexaFluor488 conjugate. This was followed by a permeabilization with −20°C methanol for 10min at 4°C, incubation with the same primary mouse anti-PfCSP, washing thrice with PBS, and incubation with a secondary goat anti-mouse AlexaFluor594 conjugate. This second step labels both intracellular and extracellular sporozoites. In case of MPCCs, the samples were counterstained with Hoechst and mounted on glass slides as described above. The number of invaded sporozoites (only green) in primary human hepatocytes were counted using Acumen Explorer.

Gliding assay

Motility of cryopreserved sporozoites was determined in each batch to define the number of infective sporozoites. Sporozoite gliding was evaluated with 20,000 sporozoites for 40 minutes in complete DMEM, at 37°C on glass cover slips covered with anti-circumsporozoite protein (CSP) monoclonal antibody (clone 2A10 for *P. falciparum* and 210 clone NSV3 for *P. vivax*). Sporozoites were subsequently fixed in 4% paraformaldehyde (PFA) for 10 minutes and stained with anti-CSP. The percentage of sporozoites associated with CSP trails was visualized by fluorescence microscopy. Quantification was performed by counting the average percentage of sporozoites that perform at least one circle.

Primaquine treatment of *P. falciparum* EEFs in MPCCs

Infected MPCCs were incubated with media containing primaquine diphosphate (Sigma) ranging from 0.5-20 μM. Fresh primaquine-containing medium was added daily until the samples were fixed at days 3 and 5 post-infection.

RNA Isolation and LMA-Luminex Analysis

Total RNA from three wells per condition was purified using Trizol (Invitrogen) and Mini-RNeasy kit (Qiagen) and pooled for analysis. LMA-Luminex procedures and probes are previously described (Chen et al., 2011). Briefly, data for triplicate loadings, expressed in mean fluorescent intensity of at least 100 beads per sample, were scaled to the human transferrin gene and row-normalized for heatmap representation using Gene Pattern open-source software (Broad Institute).

Image Automation

Images of 96 well plates were acquired using high content screening microscopes (Molecular Devices IXM), and were then analyzed by Cell Profiler and Cell Profiler Analyst (Broad Institute) (Carpenter et al., 2006; Jones et al., 2008). Parasites were visualized through immunofluorescent staining of the HSP70 protein, and can be distinguished from imaging artifacts by their proximity to a hepatocyte nucleus (within 30 pixels), and lack of auto fluorescence (no signal in unlabeled channels). We developed an automated image analysis pipeline to identify every infection in every image and measure hundreds of features (e.g. shape, area, texture) of each parasite. These features are then used to train machine learning algorithms to identify and count the number of parasites in each image using CellProfiler Analyst.

Supplementary Material

Refer to Web version on PubMed Central for supplementary material.

Acknowledgments

We thank the Malaria Research and Reference Reagent Resource Center (MRA-16, PvMSP-1/19 rabbit antiserum), deposited by (JH Adams, USF); New York University for the monoclonal antibody, 2A10; NIAID, NIH for R217; Dr. R. Wirtz, Centers for Disease Control and Prevention, and Dr. F. Zavala, Johns Hopkins University for PvCSP and HSP70 monoclonal antibodies, respectively. We are grateful to the Sanaria Manufacturing Team for the production of PfSPZ and PvSPZ. R. Schwartz for confocal microscopy help, S. Suresh and M. Diez for aid in establishing RBC cocultures, and A. Rodriguez (NYU), D. Wirth and E. Lund (HSPH) for providing mosquitoes infected with *P. yoelii and berghei*, J. Prachumsri (Mahidol Vivax Research Center) and J. Adams (University South Florida) for providing fresh *P. vivax*, H. Green (Harvard) for providing J2-3T3 fibroblasts, and H. Fleming for manuscript editing. PvSPZ production was supported by a grant from Medicines for Malaria Venture, and PfSPZ production was supported by a Phase II NIAID, NIH Small Business Innovative Research Grant (2R44A1055229) awarded to SLH. Software improvements were supported by an NIH grant (R01GM089652) to AEC. This work was supported by the Bill & Melinda Gates Foundation (Award #51066). SN is supported by an A*STAR (Agency for Science, Technology and Research, Singapore) NSS. SNB is an HHMI Investigator. The authors wish to dedicate this paper to the memory of Officer Sean Collier, for his caring service to the MIT community and for his sacrifice.

REFERENCES

Albuquerque SS, Carret C, Grosso AR, Tarun AS, Peng X, Kappe SH, Prudencio M, Mota MM. Host cell transcriptional profiling during malaria liver stage infection reveals a coordinated and sequential set of biological events. BMC Genomics. 2009; 10:270. [PubMed: 19534804]

Alonso PL, Ballou R, Brown G, Chitnis C, Loucq C, Moorthy V, Saul A, Wirth D. A research agenda for malaria eradication: vaccines. PLoS Med. 2011a; 8:e1000398. [PubMed: 21311586]

Alonso PL, Djimde A, Kremsner P, Magill A, Milman J, Najera J, Plowe CV, Rabinovich R, Wells T, Yeung S. A research agenda for malaria eradication: drugs. PLoS Med. 2011b; 8:e1000402. [PubMed: 21311580]

Annoura T, Ploemen IH, van Schaijk BC, Sajid M, Vos MW, van Gemert GJ, Chevalley-Maurel S, Franke-Fayard BM, Hermsen CC, Gego A, et al. Assessing the adequacy of attenuation of genetically modified malaria parasite vaccine candidates. Vaccine. 2012; 30:2662–2670. [PubMed: 22342550]

Bhatia SN, Balis UJ, Yarmush ML, Toner M. Effect of cell-cell interactions in preservation of cellular phenotype: cocultivation of hepatocytes and nonparenchymal cells. FASEB J. 1999; 13:1883–1900. [PubMed: 10544172]

Carlton JM, Angiuoli SV, Suh BB, Kooij TW, Pertea M, Silva JC, Ermolaeva MD, Allen JE, Selengut JD, Koo HL, et al. Genome sequence and comparative analysis of the model rodent malaria parasite Plasmodium yoelii yoelii. Nature. 2002; 419:512–519. [PubMed: 12368865]

Carpenter AE, Jones TR, Lamprecht MR, Clarke C, Kang IH, Friman O, Guertin DA, Chang JH, Lindquist RA, Moffat J, et al. CellProfiler: image analysis software for identifying and quantifying cell phenotypes. Genome Biol. 2006; 7:R100. [PubMed: 17076895]

Chattopadhyay R, Velmurugan S, Chakiath C, Andrews Donkor L, Milhous W, Barnwell JW, Collins WE, Hoffman SL. Establishment of an in vitro assay for assessing the effects of drugs on the liver stages of Plasmodium vivax malaria. PLoS One. 2010; 5:e14275. [PubMed: 21151554]

Chen AA, Thomas DK, Ong LL, Schwartz RE, Golub TR, Bhatia SN. Humanized mice with ectopic artificial liver tissues. Proc Natl Acad Sci U S A. 2011

Cogswell FB. The hypnozoite and relapse in primate malaria. Clin Microbiol Rev. 1992; 5:26–35. [PubMed: 1735093]

Conteh S, Chattopadhyay R, Anderson C, Hoffman SL. Plasmodium yoelii-infected A. stephensi inefficiently transmit malaria compared to intravenous route. PLoS One. 2010; 5:e8947. [PubMed: 20126610]

Dao NV, Cuong BT, Ngoa ND, Thuy le TT, The ND, Duy DN, Dai B, Thanh NX, Chavchich M, Rieckmann KH, et al. Vivax malaria: preliminary observations following a shorter course of treatment with artesunate plus primaquine. Trans R Soc Trop Med Hyg. 2007; 101:534–539. [PubMed: 17368694]

Durante Mangoni E, Severini C, Menegon M, Romi R, Ruggiero G, Majori G. Case report: An unusual late relapse of Plasmodium vivax malaria. Am J Trop Med Hyg. 2003; 68:159–160. [PubMed: 12641405]

Epiphanio S, Mikolajczak SA, Goncalves LA, Pamplona A, Portugal S, Albuquerque S, Goldberg M, Rebelo S, Anderson DG, Akinc A, et al. Heme oxygenase-1 is an anti-inflammatory host factor that promotes murine plasmodium liver infection. Cell Host Microbe. 2008; 3:331–338. [PubMed: 18474360]

Epstein JE, Tewari K, Lyke KE, Sim BK, Billingsley PF, Laurens MB, Gunasekera A, Chakravarty S, James ER, Sedegah M, et al. Live Attenuated Malaria Vaccine Designed to Protect through Hepatic CD8+ T Cell Immunity. Science. 2011

Gamo FJ, Sanz LM, Vidal J, de Cozar C, Alvarez E, Lavandera JL, Vanderwall DE, Green DV, Kumar V, Hasan S, et al. Thousands of chemical starting points for antimalarial lead identification. Nature. 2010; 465:305–310. [PubMed: 20485427]

Garnham PC, Bray RS, Bruce-Chwatt LJ, Draper CC, Killick-Kendrick R, Sergiev PG, Tiburskaja NA, Shute PG, Maryon M. A strain of Plasmodium vivax characterized by prolonged incubation: morphological and biological characteristics. Bull World Health Organ. 1975; 52:21–32. [PubMed: 764993]

Guguen-Guillouzo C, Guillouzo A. General review on in vitro hepatocyte models and their applications. Methods Mol Biol. 2010; 640:1–40. [PubMed: 20645044]

Guiguemde WA, Shelat AA, Bouck D, Duffy S, Crowther GJ, Davis PH, Smithson DC, Connelly M, Clark J, Zhu F, et al. Chemical genetics of Plasmodium falciparum. Nature. 2010; 465:311–315. [PubMed: 20485428]

Hoffman SL, Billingsley PF, James E, Richman A, Loyevsky M, Li T, Chakravarty S, Gunasekera A, Chattopadhyay R, Li M, et al. Development of a metabolically active, non-replicating sporozoite vaccine to prevent Plasmodium falciparum malaria. Hum Vaccin. 2010; 6:97–106. [PubMed: 19946222]

Hoffman SL, Isenbarger D, Long GW, Sedegah M, Szarfman A, Waters L, Hollingdale MR, van der Meide PH, Finbloom DS, Ballou WR. Sporozoite vaccine induces genetically restricted T cell elimination of malaria from hepatocytes. Science. 1989; 244:1078–1081. [PubMed: 2524877]

Hollingdale MR, Collins WE, Campbell CC. In vitro culture of exoerythrocytic parasites of the North Korean strain of Plasmodium vivax in hepatoma cells. Am J Trop Med Hyg. 1986; 35:275–276. [PubMed: 3006528]

Hollingdale MR, Leland P, Schwartz AL. In vitro cultivation of the exoerythrocytic stage of Plasmodium berghei in a hepatoma cell line. Am J Trop Med Hyg. 1983; 32:682–684. [PubMed: 6349397]

Jiang G, Shi M, Conteh S, Richie N, Banania G, Geneshan H, Valencia A, Singh P, Aguiar J, Limbach K, et al. Sterile protection against Plasmodium knowlesi in rhesus monkeys from a malaria vaccine: comparison of heterologous prime boost strategies. PLoS One. 2009; 4:e6559. [PubMed: 19668343]

Jones CT, Catanese MT, Law LM, Khetani SR, Syder AJ, Ploss A, Oh TS, Schoggins JW, MacDonald MR, Bhatia SN, et al. Real-time imaging of hepatitis C virus infection using a fluorescent cell-based reporter system. Nat Biotechnol. 2010; 28:167–171. [PubMed: 20118917]

Jones TR, Kang IH, Wheeler DB, Lindquist RA, Papallo A, Sabatini DM, Golland P, Carpenter AE. CellProfiler Analyst: data exploration and analysis software for complex image-based screens. BMC Bioinformatics. 2008; 9:482. [PubMed: 19014601]

Karnasuta C, Pavanand K, Chantakulkij S, Luttiwongsakorn N, Rassamesoraj M, Laohathai K, Webster HK, Watt G. Complete development of the liver stage of Plasmodium falciparum in a human hepatoma cell line. Am J Trop Med Hyg. 1995; 53:607–611. [PubMed: 8561262]

Khetani SR, Bhatia SN. Microscale culture of human liver cells for drug development. Nat Biotechnol. 2008; 26:120–126. [PubMed: 18026090]

Krotoski WA, Collins WE, Bray RS, Garnham PC, Cogswell FB, Gwadz RW, Killick-Kendrick R, Wolf R, Sinden R, Koontz LC, et al. Demonstration of hypnozoites in sporozoite-transmitted Plasmodium vivax infection. Am J Trop Med Hyg. 1982; 31:1291–1293. [PubMed: 6816080]

Krotoski WA, Garnham PC, Cogswell FB, Collins WE, Bray RS, Gwasz RW, Killick-Kendrick R, Wolf RH, Sinden R, Hollingdale M, et al. Observations on early and late post-sporozoite tissue stages in primate malaria. IV. Pre-erythrocytic schizonts and/or hypnozoites of Chesson and North Korean strains of Plasmodium vivax in the chimpanzee. Am J Trop Med Hyg. 1986; 35:263–274. [PubMed: 3513645]

LeCluyse EL, Witek RP, Andersen ME, Powers MJ. Organotypic liver culture models: meeting current challenges in toxicity testing. Crit Rev Toxicol. 2012; 42:501–548. [PubMed: 22582993]

Mazier D, Beaudoin RL, Mellouk S, Druilhe P, Texier B, Trosper J, Miltgen F, Landau I, Paul C, Brandicourt O, et al. Complete development of hepatic stages of Plasmodium falciparum in vitro. Science. 1985; 227:440–442. [PubMed: 3880923]

Mazier D, Landau I, Druilhe P, Miltgen F, Guguen-Guillouzo C, Baccam D, Baxter J, Chigot JP, Gentilini M. Cultivation of the liver forms of Plasmodium vivax in human hepatocytes. Nature. 1984; 307:367–369. [PubMed: 6363939]

McCutchan TF, Lal AA, de la Cruz VF, Miller LH, Maloy WL, Charoenvit Y, Beaudoin RL, Guerry P, Wistar R Jr. Hoffman SL, et al. Sequence of the immunodominant epitope for the surface protein on sporozoites of Plasmodium vivax. Science. 1985; 230:1381–1383. [PubMed: 2416057]

Meis JF, Rijntjes PJ, Verhave JP, Ponnudurai T, Hollingdale MR, Yap SH. Infection of cryopreserved adult human hepatocytes with Plasmodium falciparum sporozoites. Cell Biol Int Rep. 1985; 9:976. [PubMed: 3905021]

Mota MM, Pradel G, Vanderberg JP, Hafalla JC, Frevert U, Nussenzweig RS, Nussenzweig V, Rodriguez A. Migration of Plasmodium sporozoites through cells before infection. Science. 2001; 291:141–144. [PubMed: 11141568]

Mueller AK, Labaied M, Kappe SH, Matuschewski K. Genetically modified Plasmodium parasites as a protective experimental malaria vaccine. Nature. 2005; 433:164–167. [PubMed: 15580261]

Nardin EH, Nussenzweig V, Nussenzweig RS, Collins WE, Harinasuta KT, Tapchaisri P, Chomcharn Y. Circumsporozoite proteins of human malaria parasites Plasmodium falciparum and Plasmodium vivax. J Exp Med. 1982; 156:20–30. [PubMed: 7045272]

Ploss A, Khetani SR, Jones CT, Syder AJ, Trehan K, Gaysinskaya VA, Mu K, Ritola K, Rice CM, Bhatia SN. Persistent hepatitis C virus infection in microscale primary human hepatocyte cultures. Proc Natl Acad Sci U S A. 2010; 107:3141–3145. [PubMed: 20133632]

Plowe CV, Alonso P, Hoffman SL. The potential role of vaccines in the elimination of falciparum malaria and the eventual eradication of malaria. J Infect Dis. 2009; 200:1646–1649. [PubMed: 19877844]

Price RN, Tjitra E, Guerra CA, Yeung S, White NJ, Anstey NM. Vivax malaria: neglected and not benign. Am J Trop Med Hyg. 2007; 77:79–87. [PubMed: 18165478]

Prudencio M, Rodrigues CD, Hannus M, Martin C, Real E, Goncalves LA, Carret C, Dorkin R, Rohl I, Jahn-Hoffmann K, et al. Kinome-wide RNAi screen implicates at least 5 host hepatocyte kinases in Plasmodium sporozoite infection. PLoS Pathog. 2008; 4:e1000201. [PubMed: 18989463]

Pybus BS, Sousa JC, Jin X, Ferguson JA, Christian RE, Barnhart R, Vuong C, Sciotti RJ, Reichard GA, Kozar MP, et al. CYP450 phenotyping and accurate mass identification of metabolites of the 8-aminoquinoline, anti-malarial drug primaquine. Malar J. 2012; 11:259. [PubMed: 22856549]

Renia L, Miltgen F, Charoenvit Y, Ponnudurai T, Verhave JP, Collins WE, Mazier D. Malaria sporozoite penetration. A new approach by double staining. J Immunol Methods. 1988; 112:201–205. [PubMed: 3047262]

Rodrigues CD, Hannus M, Prudencio M, Martin C, Goncalves LA, Portugal S, Epiphanio S, Akinc A, Hadwiger P, Jahn-Hofmann K, et al. Host scavenger receptor SR-BI plays a dual role in the establishment of malaria parasite liver infection. Cell Host Microbe. 2008; 4:271–282. [PubMed: 18779053]

Sattabongkot J, Yimamnuaychoke N, Leelaudomlipi S, Rasameesoraj M, Jenwithisuk R, Coleman RE, Udomsangpetch R, Cui L, Brewer TG. Establishment of a human hepatocyte line that supports in vitro development of the exo-erythrocytic stages of the malaria parasites Plasmodium falciparum and P. vivax. Am J Trop Med Hyg. 2006; 74:708–715. [PubMed: 16687667]

Shortt HE, Fairley NH, Covell G, Shute PG, Garnham PC. The pre-erythrocytic stage of Plasmodium falciparum. Trans R Soc Trop Med Hyg. 1951; 44:405–419. [PubMed: 14817818]

Shortt HE, Garnham PC. The pre-erythrocytic development of Plasmodium cynomolgi and Plasmodium vivax. Trans R Soc Trop Med Hyg. 1948; 41:785–795. [PubMed: 18865442]

Silvie O, Franetich JF, Boucheix C, Rubinstein E, Mazier D. Alternative invasion pathways for Plasmodium berghei sporozoites. Int J Parasitol. 2007; 37:173–182. [PubMed: 17112526]

Silvie O, Franetich JF, Charrin S, Mueller MS, Siau A, Bodescot M, Rubinstein E, Hannoun L, Charoenvit Y, Kocken CH, et al. A role for apical membrane antigen 1 during invasion of hepatocytes by Plasmodium falciparum sporozoites. J Biol Chem. 2004; 279:9490–9496. [PubMed: 14676185]

Silvie O, Rubinstein E, Franetich JF, Prenant M, Belnoue E, Renia L, Hannoun L, Eling W, Levy S, Boucheix C, et al. Hepatocyte CD81 is required for Plasmodium falciparum and Plasmodium yoelii sporozoite infectivity. Nat Med. 2003; 9:93–96. [PubMed: 12483205]

van Schaijk BC, Janse CJ, van Gemert GJ, van Dijk MR, Gego A, Franetich JF, van de Vegte-Bolmer M, Yalaoui S, Silvie O, Hoffman SL, et al. Gene disruption of Plasmodium falciparum p52 results in attenuation of malaria liver stage development in cultured primary human hepatocytes. PLoS One. 2008; 3:e3549. [PubMed: 18958160]

Vaughan AM, Mikolajczak SA, Wilson EM, Grompe M, Kaushansky A, Camargo N, Bial J, Ploss A, Kappe SH. Complete Plasmodium falciparum liver-stage development in liver-chimeric mice. J Clin Invest. 2012; 122:3618–3628. [PubMed: 22996664]

Wang WW, Khetani SR, Krzyzewski S, Duignan DB, Obach RS. Assessment of a micropatterned hepatocyte coculture system to generate major human excretory and circulating drug metabolites. Drug Metab Dispos. 2010; 38:1900–1905. [PubMed: 20595376]

Wells TN, Burrows JN, Baird JK. Targeting the hypnozoite reservoir of Plasmodium vivax: the hidden obstacle to malaria elimination. Trends Parasitol. 2010; 26:145–151. [PubMed: 20133198]

World Health Organization. Global Malaria Programme. World Malaria Report 2010; World Health Organization: 2010.

Yalaoui S, Huby T, Franetich JF, Gego A, Rametti A, Moreau M, Collet X, Siau A, van Gemert GJ, Sauerwein RW, et al. Scavenger receptor BI boosts hepatocyte permissiveness to Plasmodium infection. Cell Host Microbe. 2008; 4:283–292. [PubMed: 18779054]

Yokoo H, Kondo T, Fujii K, Yamada T, Todo S, Hirohashi S. Proteomic signature corresponding to alpha fetoprotein expression in liver cancer cells. Hepatology. 2004; 40:609–617. [PubMed: 15349899]

HIGHLIGHTS

- Established human malaria liver stage culture using cryopreserved components (MPCC)
- MPCC recapitulates full *P. falciparum* liver stage, merozoite release and RBC infection
- MPCC allows establishment and detection of small forms in late liver stages of *P. vivax*
- MPCC's potential for anti-malarial drug screening and vaccine development validated

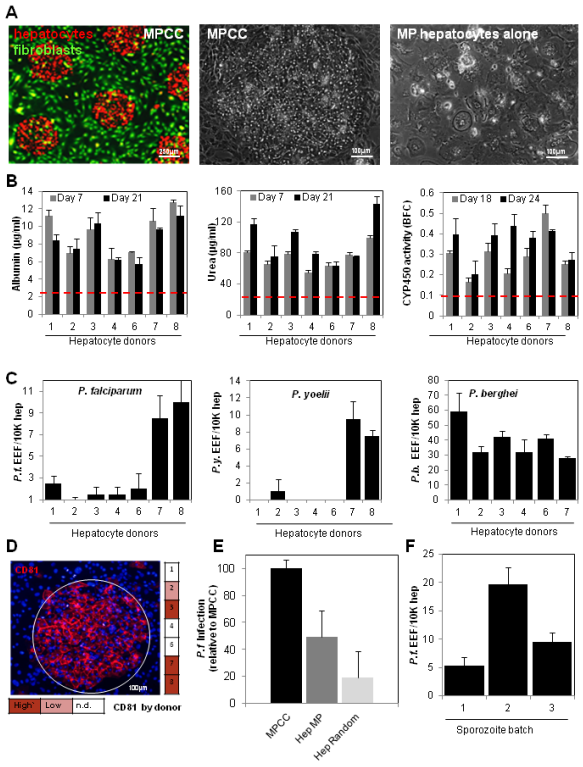

Figure 1. Functional characterization of cryopreserved human hepatocytes in micropatterned cocultures and cryopreserved *Plasmodium falciparum* sporozoites

(A) Morphology of primary human hepatocytes in micropatterned cocultures (left; hepatocytes, red and fibroblasts, green). Representative coculture of hepatocytes with (middle) and without fibroblasts (right) 18 days post-seeding. **(B)** Albumin secretion, urea synthesis and CYP450 activity in MPCC cultures of different donors. Red dashed lines indicate average levels readout in 6-day hepatocyte monocultures (stdev: 0.9, 5.4 and 0.06, respectively) **(C)** *P. falciparum, P. yoelii* and *P. berghei* infection across donors. **(D)** Representative CD81 immunofluorescence staining at day 4 post-seeding (left); heat map indicates relative CD81 expression per donor, as measured by IF (right; n.d, not detected) **(E)** *P. falciparum* infection in hepatocyte monocultures, micropattern (MP) or randomly distributed (Random), relative to infection in MPCCs. 10K hepatocytes were plated in each case **(F)** Levels of infection by three sporozoite batches in a single hepatocyte donor. See also Figure S1. Error bars represent standard deviation (stdev). See also Figure S1.

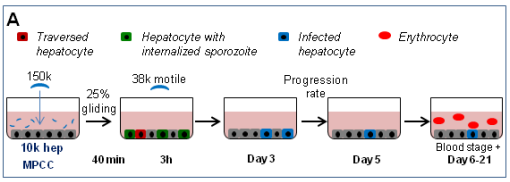

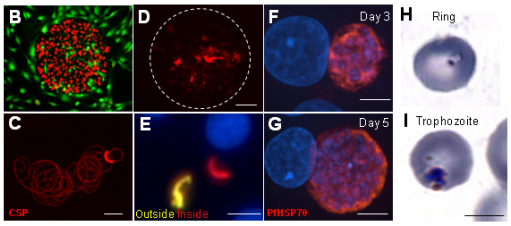

J

Infection rates based on	MPCC		HC04	
	Percent invasion and development		Percent invasion and development	
	3-Day Assay (*HSP70*)	6-Day Assay (*MSP1*)	3-Day Assay (*HSP70*)	6-Day Assay (*MSP1*)
Hepatocyte (E_h)	0.18	0.06	0.14	0.02
Sporozoite (E_s)	0.03	0.01	1.16	0.08

E_h: # of infected hepatocytes/hepatocytes; E_s: # of spz that infect/total # of viable spz

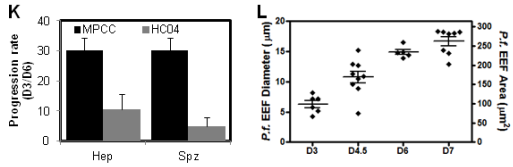

Figure 2. Liver stage recapitulation in primary human hepatocyte MPCCs

(A) Schematic of *P. falciparum* infection assay. **(B)** Typical morphology of primary human hepatocytes in MPCC (hepatocytes, red; fibroblasts, green). **(C)** Representative image of *P. falciparum* sporozoites gliding. CSP immunostaining used to visualize trails. Quantification based on the average fraction of sporozoites that perform at least one circle. **(D)** Cell traversal ability of *P. falciparum* sporozoites as visualized by dextran-positive staining of primary human hepatocytes. **(E)** Representative double immunofluorescence stain (anti-PfCSP, both before and after cell permeablization) of *P. falciparum* infected MPCCs. Extracellular and intracellular sporozoites are labeled yellow and red, respectively. Nuclei visible with blue DAPI stain. **(F, G)** Representative images of *P. falciparum* in human primary hepatocytes at day 3 and 5 post-infection. Parasites are identified by anti-PfHSP70 staining (red). **(H,I)** Infection of human RBCs by merozoites released from infected liver stage culture. Representative images of Giemsa-stained RBCs in the ring stage (H), and the trophozoite stage (I). **(J)** Infection rates using MPCC primary human hepatocytes or HC04 hepatoma cells, calculated based on the plated number of sporozoites or hepatocytes. **(K)** Progression rate from day 3 to day 6 in MPCC and HC04 calculated as: Infection rate day 6/ infection rate day 3 × 100 (based on hepatocytes and sporozoites) **(L)** Schizont size distribution at day 3, 4.5, 6 and 7. Scale bar: 5µm (F-I), 10µm (C,E), 100µm (D). Error bars represent standard error of the mean (SEM).

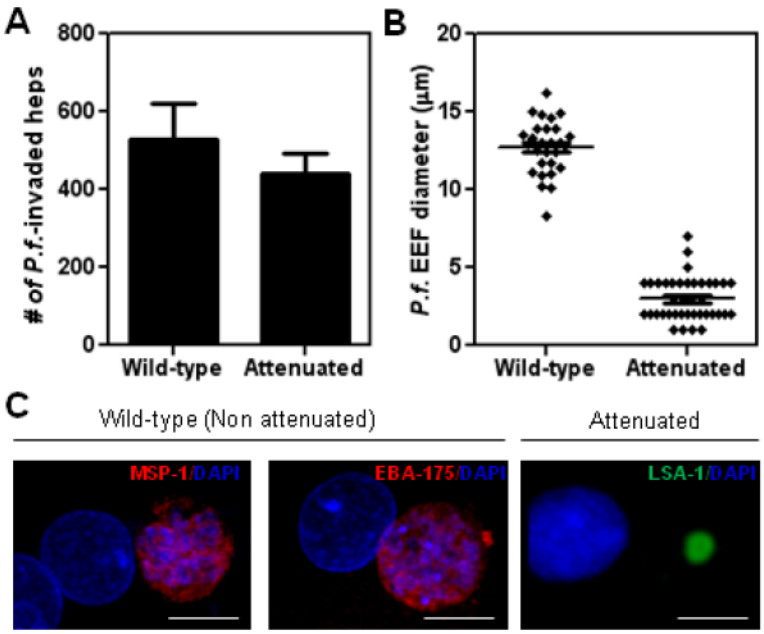

Figure 3. Comparison of live attenuated versus wild-type parasite for candidate vaccine evaluation

(A) Number of infected hepatocytes observed after wild-type (non-attenuated) and attenuated cryopreserved sporozoites infection **(B)** Size distribution of wild-type and attenuated parasites in MPCC after five days of culture. **(C)** Representative images of parasites at day 5 post infection. Wild-type parasites are identified by anti-MSP-1 and anti-EBA-175 staining. Attenuated parasites are identified by anti-LSA-1 staining. Nuclei are visualized with DAPI (blue). Scale bar: 10µm. Error bars represent standard error of the mean (SEM).

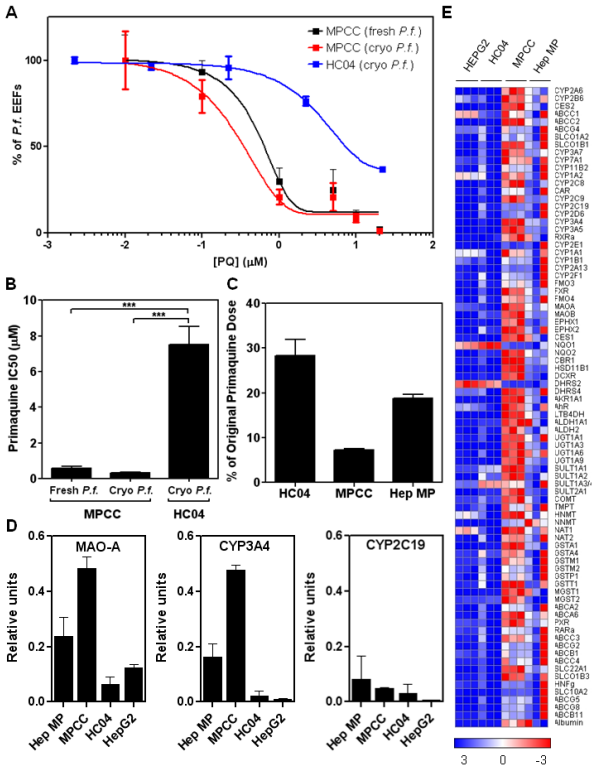

Figure 4. Utility of medium-throughput human hepatocyte platform to identify lead compounds

(A) Primaquine treatment of MPCC or HC04 infected with fresh or cryopreserved sporozoites. **(B)** IC50 of primaquine in MPCC vs HC04 ($p = 0.0002$ by 1way ANOVA, ***$p < 0.001$ by Tukey multiple comparison test). **(C)** Primaquine metabolism by HC04, MPCC, and patterned monocultures of primary human hepatocytes (Hep MP), quantified by LC/MS/MS. **(D)** Relative expression of 3 putative metabolism genes implicated in primaquine metabolism **(E)** Heat map displays of LMA-Luminex analysis for 83 human-specific drug metabolism genes. Columns represent triplicate loadings of RNA extracted from HEPG2, HC04, MPCC and Hep MP. Gene expression relative to average of control gene transferrin, and heat maps are row-normalized. See also Figure S2. Error bars represent standard error of the mean (SEM). See also Figure S2.

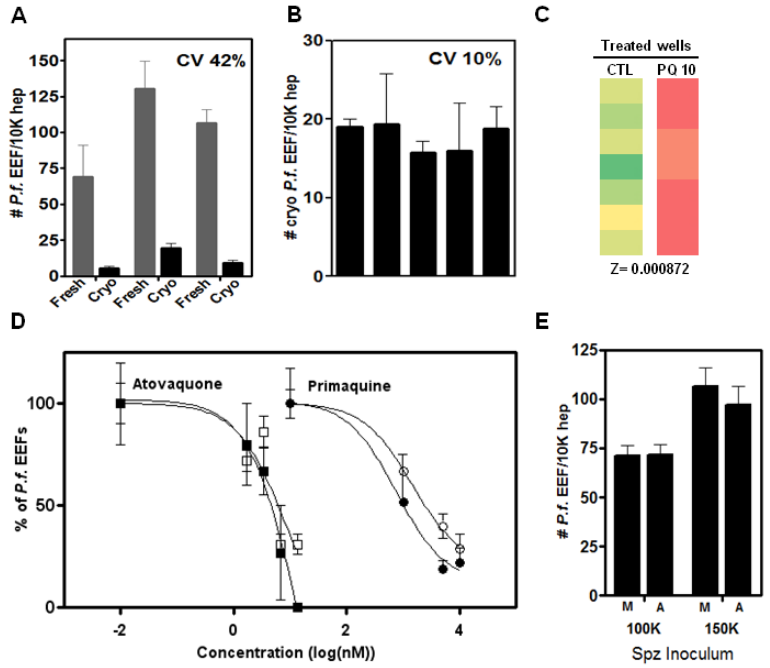

Figure 5. Adapting the format to drug screening

(A) Inter-experimental variability measured by the coefficient of variation (CV) and infection rate using fresh and cryopreserved sporozoites from three different batches. **(B)** Inter-experimental variability measured by the coefficient of variation (CV) and infection rate using cryopreserved sporozoites from the same batch. **(C)** Heat map indicating levels of infection (green, highest EEF numbers; red, lowest EEF numbers) observed in 7 representative control or primaquine treated wells. Comparison yields positive Z factor. **(D)** *P. falciparum* infection with primaquine or atovaquone in 2 independent experiments performed on different days. **(E)** *P. falciparum* infection in MPCCs following two doses of fresh sporozoites determined by manual counts (M) or by image analysis automation (A). See also Figure S3. Error bars represent standard error of the mean (SEM). See also Figure S3.

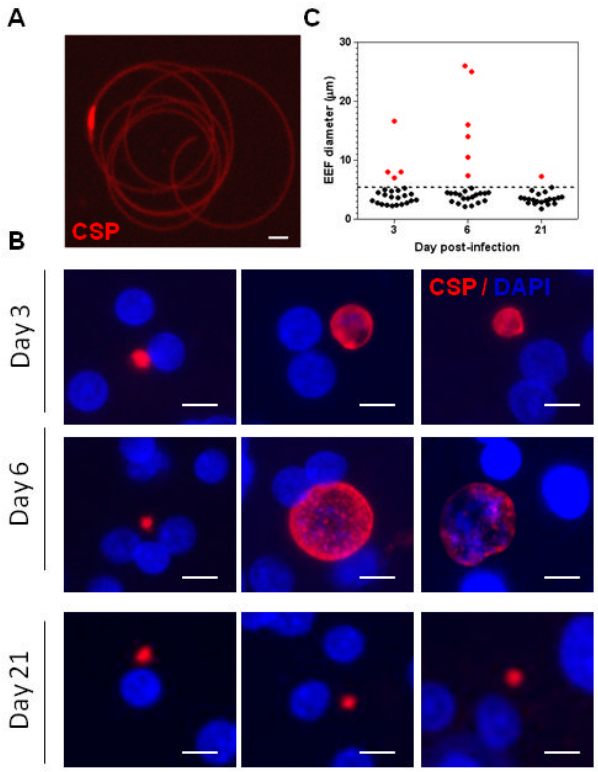

Figure 6. Infection with *Plasmodium vivax*

(A) Representative image of PvCSP-stained *P. vivax (chesson)* sporozoites gliding. **(B)** Representative images of PvCSP+ parasites over time. Scale bar: 10µm. **(C)** Size distribution of *P. vivax* parasites in MPCC over time. Red: all observed parasites bigger than 5µm; black: 20 representative small forms smaller than 5µm. See also Figure S4.